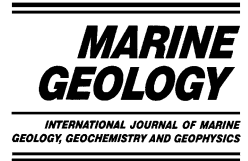




ELSEVIER

Marine Geology 195 (2003) 177–200



www.elsevier.com/locate/margeo

Vast fields of hydrocarbon-derived carbonate chimneys related to the accretionary wedge/olistostrome of the Gulf of Cádiz

V. Díaz-del-Río^{a,*}, L. Somoza^b, J. Martínez-Frias^c, M.P. Mata^d,
A. Delgado^e, F.J. Hernandez-Molina^d, R. Lunar^f, J.A. Martín-Rubí^b,
A. Maestro^b, M.C. Fernández-Puga^b, R. León^b, E. Llave^b, T. Medialdea^b,
J.T. Vázquez^d

^a Centro Oceanográfico de Málaga, Instituto Español de Oceanografía, Fuengirola, 29640 Malaga, Spain

^b Marine Geology Division, IGME Geological Survey of Spain, 28003 Madrid, Spain

^c Centro de Astrobiología, CSIC/INTA, Torrejón de Ardoz, 28850 Madrid, Spain

^d Facultad de Ciencias del Mar, Universidad de Cádiz, Puerto Real, 1510 Cádiz, Spain

^e Estacion Experimental del Zaidín, CSIC, 18008 Granada, Spain

^f Departamento de Cristalografía y Mineralogía, Universidad Complutense, 28040 Madrid, Spain

Received 2 June 2001; accepted 5 November 2002

Abstract

We report the first discovery and sampling of vast fields of hydrocarbon-derived carbonate chimneys along the Gulf of Cádiz continental slope, at depths between 500 and 1200 m. A large variety of carbonate chimneys (more than 200 samples) were recovered from four different areas, named the DIASOM, TASYO, GBF (Guadalquivir Basin) and ESF (East Moroccan) fields. Observations from an underwater camera revealed a spectacular high density of pipe-like chimneys, some of them longer than 2 m, lying over the sea floor, and some protruding from muddy sediment. Local fissures and alignment of isolated chimneys were also observed, suggesting that their distribution is controlled by fault planes. Chimneys collected show a wide range of morphological types (spiral, cylindrical, conical, mushroom-like and mounded) with numerous nodule protuberances and ramified fluid channelways. The chimneys are mainly composed of authigenic carbonates (ankerite, Fe-bearing dolomite and calcite) with abundance of iron oxides, forming agglomerates of pseudo-pyrite framboids. $\delta^{18}\text{O}$ isotopic values vary from 0.7 to 5.5‰ whereas $\delta^{13}\text{C}$ values indicate that chimney carbonates are moderately depleted in ^{13}C , ranging from -46‰ to -20‰ PDB, interpreted as formed from a mixture of deep thermogenic hydrocarbons and shallow biogenic methane. These vast fields of carbonate chimneys imply new considerations on the importance of hydrocarbon fluid venting in the Gulf of Cádiz and, moreover, on the active role of the olistostrome/accretionary wedge of the Gibraltar arc.

© 2003 Elsevier Science B.V. All rights reserved.

Keywords: carbonate chimneys; mounds; hydrocarbon seeps; microbial chemosynthesis; accretionary wedges, Gulf of Cádiz

1. Introduction

In the last years, numerous studies of modern submarine environments and rocks of the fossil

* Corresponding author.

E-mail address: diazdelrio@ma.ieo.es (V. Díaz-del-Río).

record have stressed the importance of carbonate formation associated with hydrocarbon seepage and bacterial activity (e.g. Camoin, 1999). In recent submarine environments, carbonate and barite chimneys, slabs and crusts associated with hydrocarbon seeps have been reported in various tectonic settings: Oregon margin (Schroeder et al., 1987); North Sea (Hovland et al., 1987; Hovland and Judd, 1988); Gulf of Mexico (Baoshum et al., 1994; Roberts and Carney, 1997); Monterey Bay (Orange et al., 1999; Stakes et al., 1999); Kattgat (Jørgensen, 1992); Nankai Trough (Sakai et al., 1992), Otago continental slope, southern New Zealand (Orpin, 1997) and Makran accretionary wedge (Von Rad et al., 1996).

In the Gulf of Cádiz, pockmark-like structures on the shelf break (Baraza and Ercilla, 1996) and mud volcanoes bearing gas hydrates, authigenic carbonate crusts and slabs discovered along the continental slope (Ivanov et al., 2000; Somoza et al., 2000; Gardner, 2001) have revealed the intense activity of hydrocarbon seeps, both on the Iberian and African margins. According to the results of gas measurements, the fluid venting areas in the Gulf of Cádiz are characterised by a relatively high background gas content (up to 292 ml/l) in comparison with other areas of extensive hydrocarbon seeps such as the Eastern Mediterranean Sea and the Black Sea (Stadnitskaia et al., 2000).

On the Iberian continental margin of the Gulf of Cádiz, a research cruise aboard the R/V *Hespérides* surveyed the continental slope with multi-beam echo-sounders and ultra-high resolution seismics. A large number of mud volcanoes, mud ridges, crater-like pockmarks, and large sediment slides were mapped. In 2000 and 2001, two research cruises aboard R/V *Cornide de Saavedra* were conducted to the targets previously identified on multibeam bathymetry and seismic surveys, using underwater camera, coring and dredging. A large field of carbonate chimneys was discovered, named DIASOM, showing an unusual high abundance and variety of pipe-like morphologies. This paper describes the first observations of a carbonate chimney field in the Gulf of Cádiz, the DIASOM field, although for the purposes of comparison and future research we have included

geochemical data from isolated chimneys found in other sites of the Gulf of Cádiz. In this way, the objectives of this contribution are to: (1) report our preliminary results on the petrography, geochemical characteristics and stable isotopic data of these vast fields of chimneys; (2) draw comparisons between previously reported hydrocarbon-related chimneys and authigenic carbonates in other areas of cold seeps; and (3) comment on the processes that may control the formation of these types of submarine structures and their relationship with bacterial activity.

2. Geological setting

The Gulf of Cádiz is located at the front of the Gibraltar arc, the westernmost tectonic belt of the Alpine–Mediterranean compressional system (Fig. 1). This front consists of the olistostrome/accretionary complex units, emplaced in the Late Miocene (Maldonado et al., 1999), in response to the NW–SE directed convergence between the African and Eurasian plates (Flinch et al., 1996). Four main tectonic allochthonous provinces surround the internal zones of the Gibraltar arc orogenic belt overlying both the Iberian and African passive margins (Fig. 1): (a) Flysch units of the Campo de Gibraltar complex; (b) external zones, tectonically detached Mesozoic sediments ranging from Lower Jurassic to Upper Cretaceous–Palaeocene pre-tectonic units; (c) Triassic Diapir Zone, composed mainly of salts, gypsum and shallow carbonate deposits emplaced as diapiric expulsion by thrusting of thick nappes of Mesozoic sediments (Berástegui et al., 1998); and (d) the front of the deformed wedge, mainly formed by plastic clays and marls of Early–Middle Miocene age (Maldonado et al., 1999).

The most frontal parts of the Gibraltar arc are composed of Triassic evaporites and Miocene plastic marls and have been referred to traditionally as the ‘Olistostrome Zone’ (Perconig, 1960–62) or ‘Gualdalquivir Allochthonous Unit’ (Blankenship, 1992) (Fig. 1). The end of the Gibraltar arc emplacement occurred during the Late Miocene, coinciding with accelerated tectonic subsi-

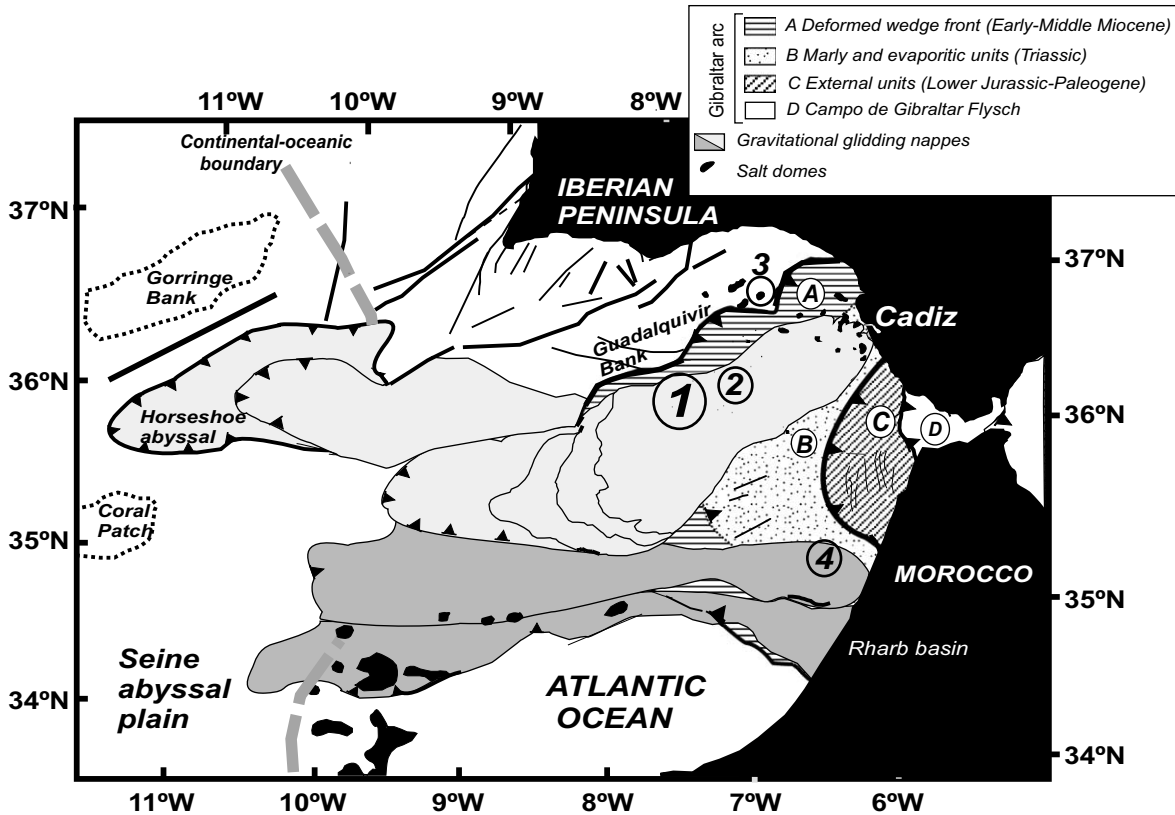


Fig. 1. Simplified structural map with tecto-sedimentary units that compose the olistostrome/accretionary wedge of the Gulf of Cádiz (modified from Somoza et al., 1999). The location of the main sites where carbonate chimneys have been recovered is indicated: (1) DIASOM field, (2) TASYO field, (3) Guadalquivir Basin Field (GBF), and (4) Eastern Moroccan field (ESF).

dence on the shelf, which resulted in gravitational gliding and spreading of Triassic salt and Miocene shale deposits towards the Central Atlantic basins (Somoza et al., 1999). Major gravitational gliding nappes have been defined in the Gulf of Cádiz, on the Spanish–Portuguese margin (Cádiz Salt Nappe) and the Moroccan margins (e.g. Rharb Basin), which were detached from the front of the olistostrome/accretionary complex (Somoza et al., 1999). The Late Miocene accretionary front has extended since the early Pliocene from the shelf towards the Horseshoe and Seine abyssal plains (Torelli et al., 1997), west to the Gibraltar arc, with thickness exceeding 2.4 km (Vázquez et al., 2001). Fault systems observed on the sea floor related to active mud volcanoes (Gardner et al., 2001) are coherent with the N-160° directed convergence between the African and Eurasian plates

proposed for the present times in the Gulf of Cádiz.

Deformation structures observed on seismic lines along the shelf and slopes of the Gulf of Cádiz provide geometric evidence for shale/salt tectonics and related hydrocarbon seepage on the sea floor (Fernández-Puga et al., 2000). Overpressured compartments generated beneath salt/shale arched wedges (Fig. 1) have been suggested as a mechanism to provide avenues for hydrocarbon gases, brines and fluidised sediments to migrate upwards through contraction toe-thrust structures (Lowrie et al., 1999).

3. Chimney fields in the Gulf of Cádiz

Carbonate chimneys found in the Gulf of Cádiz

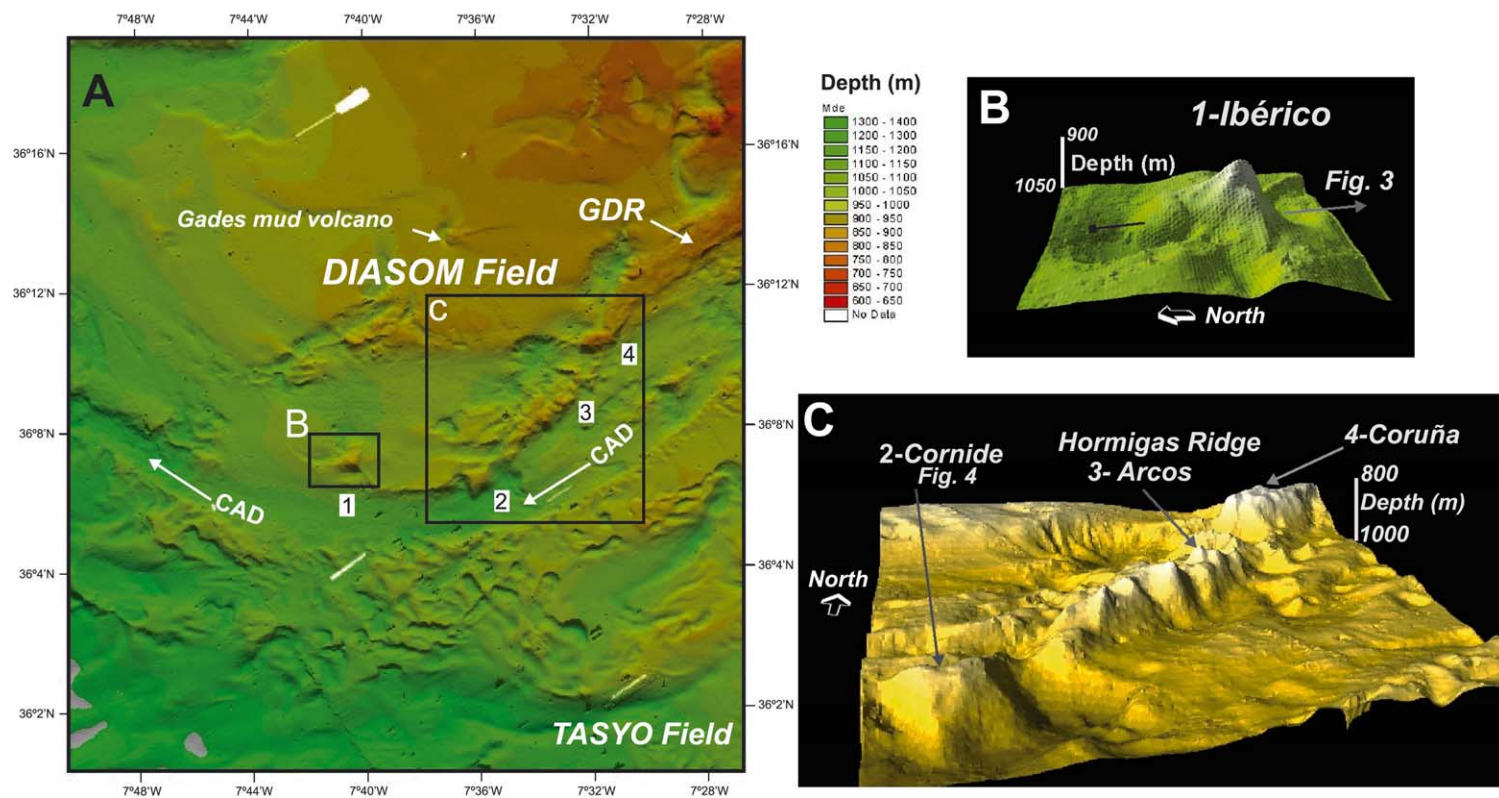


Fig. 2. (A) Multibeam bathymetry of the main study area, the DIASOM field, showing the location of the main sites where carbonate chimneys were sampled and observed by underwater camera: (1) Ibérico, (2) Cornide, (3) Arcos, and (4) Coruña. GDR is the Guadalquivir Diapiric Ridge, a NW–SE linear diapiric ridge located on the eastern side of the DIASOM field. The Cádiz undercurrent channel (CAD), is the main contourite channel of the Mediterranean outflow. Note that the sea floor morphology is mainly characterised by collapse structures and slide scar probably related to extensive gas seepage (Somoza et al., *this volume*). (B) Detailed oblique view, looking east, of the Ibérico mound. Most of the carbonate chimneys were collected on the southernmost steep flank (up to 30°) of this mound. Location of seismic profile (Fig. 3) crossing this structure is also shown. (C) Oblique view, looking northeast, of the eastern part of the DIASOM field. Carbonate chimneys were dredged and photographed on the crest of the mounds. The alignment of high-relief and small cone-shaped mounds located between Cornide and Coruña mounds has been named the Hormigas Ridge. The slopes of the southernmost side of this prominent high range between 30° and 40°. Note also the minor cone-shaped structures appearing along the CAD channel.

are associated with fields of mud volcanism and mud/salt diapirism being closely related to the above described tectono-sedimentary units (Fig. 1). The areas where carbonate chimneys have been found may be grouped as follows:

(1) The DIASOM field (Fig. 2) is composed of several mounds forming an arcuate mud ridge. The Ibérico mound was the first surveyed site, where 76 chimney samples were collected at depths ranging from 850 to 1100 m, during the Anastasya 2000 cruise. This area was intensively explored during the Anastasya 2001 cruise, leading to the discovery of large numbers of carbonate chimneys and slabs in three more mounds (Cornide, Arcos and Coruña), at depths between 1100 and 920 m. This field lies close to the deformed wedge front of the olistostrome/accretionary complex, mainly composed of plastic blue marls of Early–Middle Miocene age (Somoza et al., 2001).

(2) The TASYO field, an area of widespread fluid venting, is characterised by numerous crater-like collapse structures and mud volcanoes. Several small pipe-like carbonate chimneys associated with carbonate crusts were found along the flanks of the Hespérides mud volcano complex, at depths between 750 and 900 m. The Hespérides mud volcano is the largest structure of the TASYO field. This mud volcano is seated on a sea floor-piercing diapir, being composed of six single circular cone-shaped domes with a seabed diameter of more than 3 km and a relative height of 150 m (Somoza et al., 2003).

(3) The Eastern Moroccan field (ESF) mud volcano field is an area with extensive mud volcanism (Ivanov et al., 2000; Gardner, 2001) located within the Triassic Diapir Zone of the olistostrome/accretionary complex. Although this area has not been intensively investigated, mushroom pipe-like chimneys were found at a water depth of 450 m.

(4) The Guadalquivir Basin field (GBF) is related to Triassic salt diapirs pinching out along the front-thrusting wedges of the olistostrome/accretionary complex (Maldonado et al., 1999). In this area, not intensively investigated, a fragment of carbonate chimney was found at a water depth of 514 m.

4. Methods

4.1. Sampling and swath bathymetry

Samples were collected with a rectangular benthic-type dredge during the 2000 and 2001 R/V *Cornide de Saavedra* cruises. A standard gravity corer, 3 m long, was also used to take samples from mud sediments hosting the carbonate chimneys. Navigation was made with differential Global Positioning System (DGPS) for which the average navigational accuracy is estimated to be better than ± 5 m. Mound-shaped targets were previously detected during the 2000 R/V *Hespérides* cruise, a detailed mapping and ultra-high resolution seismic survey that produced more than 1200 km of new data on the continental slope of the Gulf of Cádiz. The Simrad EM12S-120 system is a hull-mounted multibeam echo-sounder capable of recording detailed bathymetric and backscatter data with a high resolution of tens to hundreds of metres in the horizontal and less than 5 m in the vertical direction. Operating at a frequency of 13 kHz, the EM12-120 system uses 81 beams spread over 120° to image a swath of sea floor 2.5 times the water depth in width. The swath mapping provided a bathymetric map contoured at 1 m interval as well as a subsidiary map of sea-floor backscattering of the sonar signal (León et al., 2001). The parasound echo-sounder TOPAS (Topographic Parametric Sound) seismic data obtained allowed us to identify high-reflectivity mounds related to subsurface fluid venting.

4.2. Geochemical, mineralogical and isotopic analysis

Specimens were examined in hand samples and a microscopic study on transmitted and reflected light was made. Bulk mineralogy was determined using X-ray diffraction (XRD) on powdered samples using a diffractometer with CuK α radiation (Philips PW-1700) of the Instituto Geológico y Minero de España. Scanning electron microscopic analysis was made on both carbon-coated thin sections and gold-coated fragments of chimneys, using a Philips XL20 scanning electron micro-

scope with accelerating voltages of 20–30 kV, at the Complutense University of Madrid. The chemical composition of bulk rock composition, and major and trace elements were analysed by X-ray fluorescence (Philips PW-1404) and ICP (Thermo Jarell Ash ICAP 61). Electron microprobe analyses were made on a Jeol Superprobe JXA-8900M at the Servicio de Microscopía Elec-

tronica Lluís Bru, Complutense University of Madrid.

Isotope measurements were carried out at the Stable Isotope Laboratory of the Estación Experimental del Zaidín (CSIC, Granada, Spain). Carbon dioxide was extracted from the carbonates using 100% phosphoric acid at 25°C (calcite) and 50°C (siderite). Isotopic ratios were measured

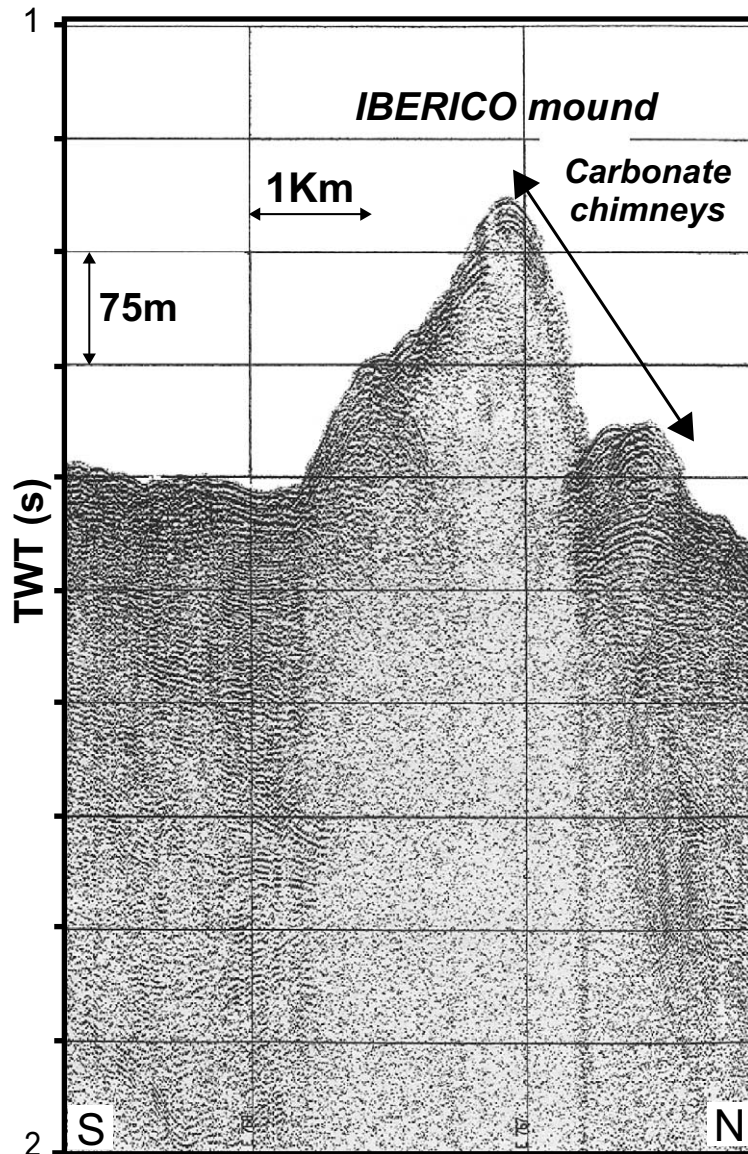


Fig. 3. N–S running seismic profile (sparker) showing the cone-shaped Ibérico mound formed by acoustically transparent facies. Most chimneys were dredged on the southern flank of this mound, characterised by a surface with a high-reflective response.

by a Finnigan MAT 251 mass spectrometer. The reproducibility of the analytical procedure was lower than $\pm 0.1\%$ for calcite and $\pm 0.2\%$ for carbonate–Fe–Mg. All the samples were compared to a reference carbon dioxide obtained from a calcite standard prepared at the same time. Thus, oxygen isotope ratios for ankerite were recalculated taking into account the fractionation factor for acid decomposition at 50°C, 1.01057 for ankerite and at 25°C, 1.01044 for calcite.

5. The DIASOM chimney field

5.1. Swath bathymetry and sea-floor observations

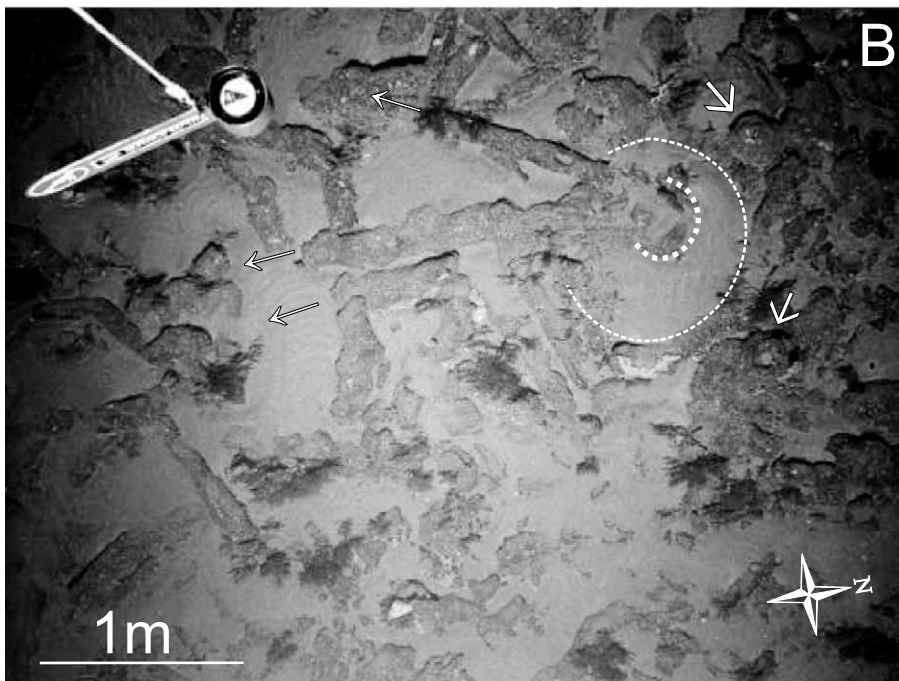
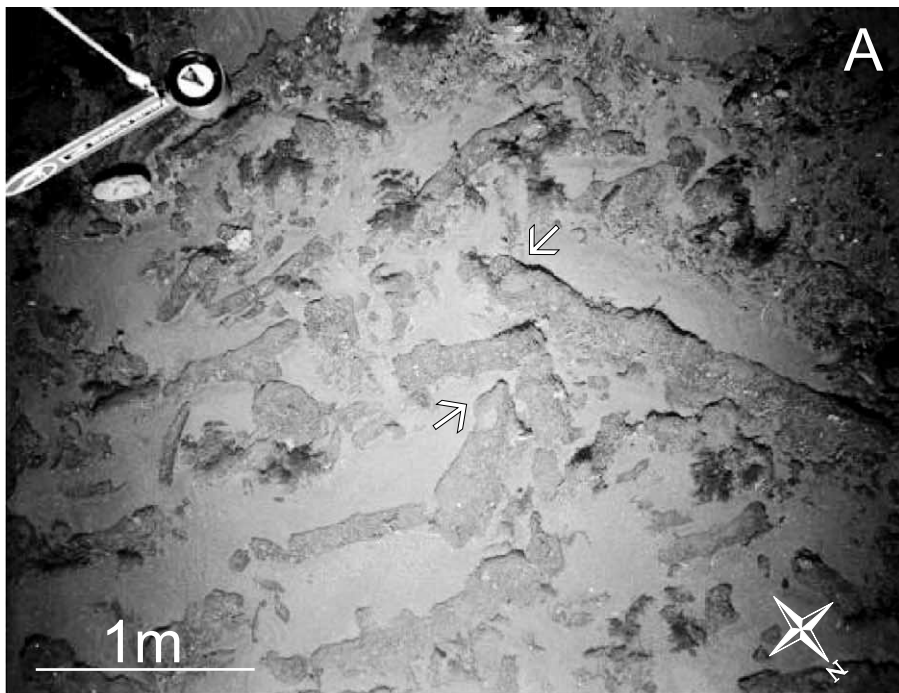
The DIASOM chimney field is a prominent structural high with steep slopes up to 25° and irregular crests at water depths between 800 and 950 m (Fig. 2). A series of cone-shaped mounds follows an arcuate-shaped ridge at the northern edge of the Cádiz valley (CAD), the largest undercurrent channel of the Mediterranean outflow (Fig. 2A). This arcuate ridge is located at the westernmost edge of the Guadalquivir Diapiric Ridge (GDR) and is likewise a linear diapiric ridge which trends NE–SW. It is formed of lower–middle Miocene plastic marls (Somoza et al., 2003). NW–SE trending faults inferred from multibeam bathymetry divide the arcuate ridge into several segments. The same fault orientation is also observed controlling active mud volcanoes on the Moroccan margin (Gardner et al., 2001). Four main sites with extensive fields of carbonate chimneys were detected and sampled (Fig. 2A): (1) the Ibérico mound, a large isolated cone at the western side of the field; (2) the Cornide mound, the largest feature of the field; (3) the Hormigas Ridge, an alignment of high-relief and small cone-shaped mounds; and (4) the Coruña mound, the easternmost mound, characterised by a flat summit.

The Ibérico mound provided the first evidence for the presence of large fields of pipe-like chimneys in the Gulf of Cádiz (Díaz-del-Río et al., 2001). It is a 870 m deep and 165 m tall cone-shaped structure, characterised by an asymmetric

profile with steep slopes of 22°–25° and 12°–15° on its southward and northward flank, respectively (Fig. 2B). A suite of more than 76 individual structures of chimneys was dredged on its southernmost flank. At the same time, dolomite slabs were also collected. Detailed multibeam bathymetry shows the mound surrounded by collapse structures and slide scars. The highly reflective surface observed on sparker seismic lines (Fig. 3) can be related to the presence of carbonate chimneys and slabs. Otherwise, chaotic and indistinct seismic reflection patterns appear in the subsurface. Small, highly reflective minor mounds are also observed on the flanks of the main mound. Video imagery at the top of the Ibérico mound obtained during the TTR-11 cruise shows large colonies of *Callogorgia verticillata*, many specimens of sea urchins, Cidaridae, and sea stars, Asterinidae (Cunha et al., 2002).

The DIASOM field was intensively investigated during the Anastasya 2001 cruise, leading to the discovery of large numbers of carbonate chimneys and slabs from three other mounds, named Cornide, Arcos and Coruña. The Cornide mound appears as the largest feature of this field (Fig. 2C). It is characterised by a flat top at 950 m depth, with an elevation of 230 m and steep flanks up to 30°, next to the Cádiz channel, the main Mediterranean outflow valley. Observations from the underwater camera revealed a high density of pipe-like chimneys and carbonate slabs over the flat top of this mound (Fig. 4). Most of the chimneys lie on the sea floor but some small chimneys protrude from muddy sediments. Coring from the top of the mound yielded ‘mousse’-like muds with indications of gas saturation and a H₂S smell.

The Arcos mound is one of the small cone-shaped mounds with steep flanks, located along the Hormigas Ridge (Fig. 2C). It is a 850 m deep and 200 m tall cone structure with steep southern flanks (max. 35°), on the margin of the Cádiz valley. Observations from the underwater camera revealed the presence of numerous pipe-like chimneys and carbonate slabs along its flanks. Some chimneys protrude from muddy sediments, although most of them are lying on the sea floor. Local fissures and alignment of isolated chimneys were also observed, suggesting that their distribu-



tion is controlled by fault planes. Many large pipe-like chimneys and slabs were collected from this site. The carbonate slabs have a thickness of 10–15 cm and some of them form the base of the pipe-like chimneys. Samples collected from the northernmost structure of the Hormigas Ridge (Fig. 2C) revealed the presence of large boulders, up to 50 cm across, of plastic blue marls, the characteristic ‘blue marls’ facies of the pre-olistostrome Early–Middle Miocene units of the olistostrome/accretionary complex (Maldonado et al., 1999). This suggests that the Hormigas Ridge is formed mainly by diapirism of the undercompacted pre-olistostrome units.

The Coruña mound is the westernmost feature along the DIASOM field, and shows characteristics similar to the Cornide structure: flat top and steep flanks. Its summit is at 820 m with a relief of 210 m above the Cádiz channel. Dredging from the top of this structure yielded abundant pipe-like carbonate chimneys and fragments of carbonate crusts. Centimetric clasts of plastic blue marls and calcarenites were also collected. At the south-eastern side of this structure, several small sub-circular cone-shaped mounds elevated from the Cádiz valley sea floor are observed on the multi-beam bathymetry (Fig. 2C), resembling single mud volcanoes observed at the eastern side of the Guadalquivir Diapiric Ridge (Somoza et al., 2003)

5.2. Types and morphologies of chimneys

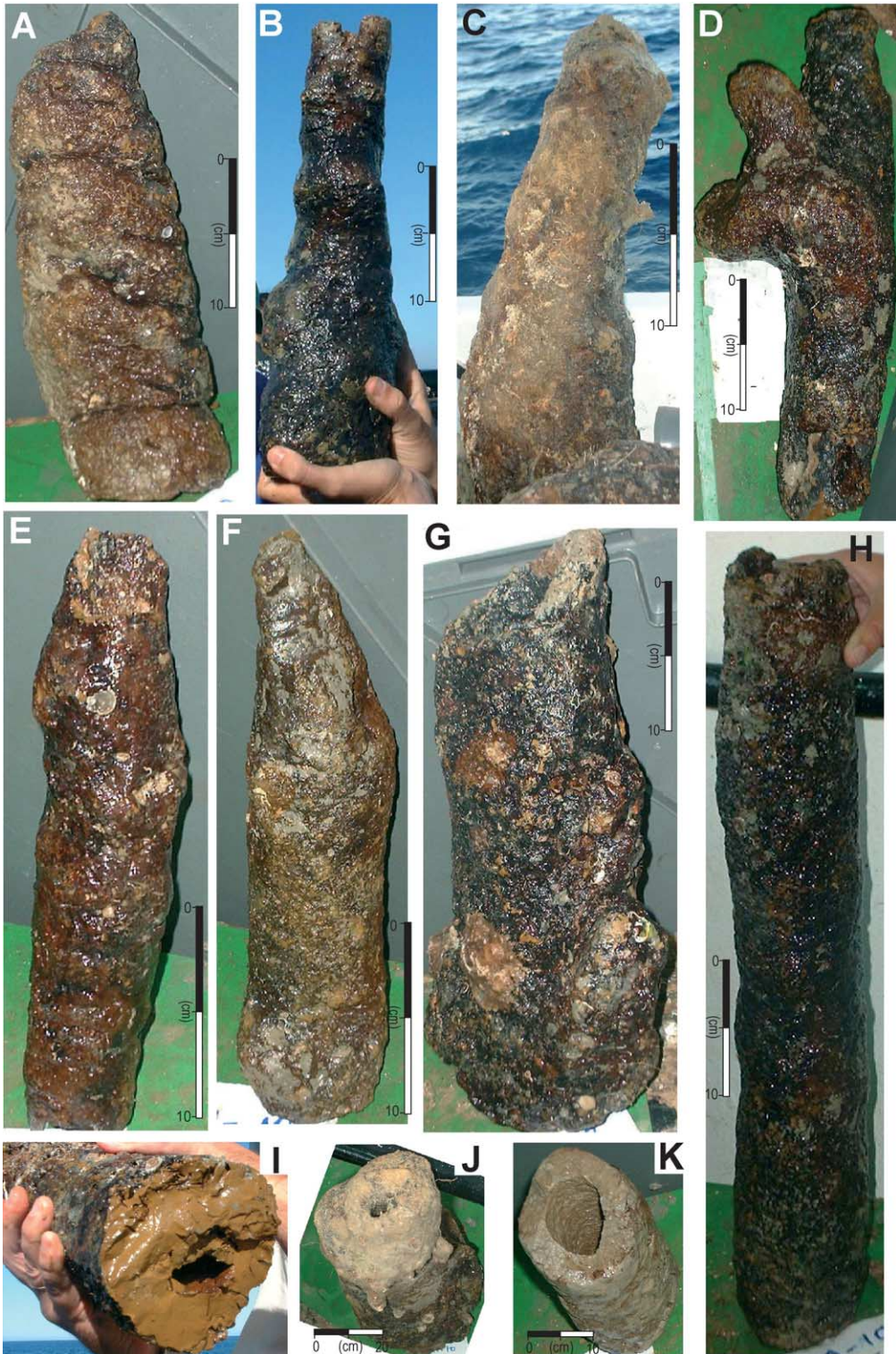
More than 200 samples of carbonate chimneys and slabs were collected in the DIASOM field. The chimneys show a wide range of morphologies (Figs. 5 and 6) and sizes (5–30 cm in diameter and 15–55 cm in length). The surface of the chimneys is often irregular with nodule protuberances and fluid channelways. Chimney tubes can be straight, tortuous, ramified, and helical (Figs. 5 and 6).

Small bifurcations of the principal vent orifice are also observed in some chimneys. Outer walls of chimneys are iron oxide-stained, having brownish red to black colours. Bryozoa and coral encrustations can also be observed in most of the samples. The walls of the chimneys can exhibit growth layers characterised by changes in colour from dark grey to light orange close to the exterior walls. In some cases, venting conduits are fully or partially filled by marly sediments. The smaller epifauna retrieved from the chimneys collected at the Iberico site is characterised by the occurrence of brachiopod clusters (*Gryphus vitreus*), encrusting sponges, and polychaetes crawling out of tiny conduits (*Pholoides dorsipapillatus*) (Cunha et al., 2002).

Cylindrical pipe-like chimneys are the most common types. The largest in size reach 14 cm in diameter with central orifices of 7 cm, and 53 cm in length. The average sizes range between 8 and 10 cm in diameter with orifices of 2–3 cm. Small pipe-like chimneys have also been found with diameters of 5 cm, with similar morphologies to the largest sizes. Two different terminations of pipe-like chimneys have also been observed: (a) bullet-like termination, showing a progressive thinning of the cylindrical pipe toward the top, and (b) mushroom-like termination, characterised by a protuberance enclosing the top of the pipe-like tubes. The conical-type chimneys are characterised by upward thinning of the tube diameter, with normal sizes of 40 cm in length, 12 cm at the base and 7 cm at their top with central orifices of 4–5 cm (Fig. 5B). The largest in size reaches 40 cm in length. Several chimneys of this type show the main vent orifice bifurcated at its top.

The third type is characterised by mound-like shapes that show the largest diameters observed in all the samples, with a wide basal diameter of 21 cm, decreasing to 13 cm toward the top. This type also shows thick outer walls up to 21 cm in

Fig. 4. Bottom photographs of the carbonate chimneys taken with a BENTHOS underwater camera along the crest of the Cornide mound, at depths between 950 and 970 m. See Fig. 2C for location. (A) Large carbonate chimneys, some longer than 1.5 m, lying on the sea floor. Note the high abundance of chimneys at this site. The field of view is about 3 m across. (B) Large chimneys falling southwards and radially from a sub-circular structure, probably the feeder channel. This suggests the formation of several chimneys from the same conduit. Note also minor chimneys protruding vertically from the sea floor. Carbonate slabs underlie superficial sandy sediments with ripple marks.



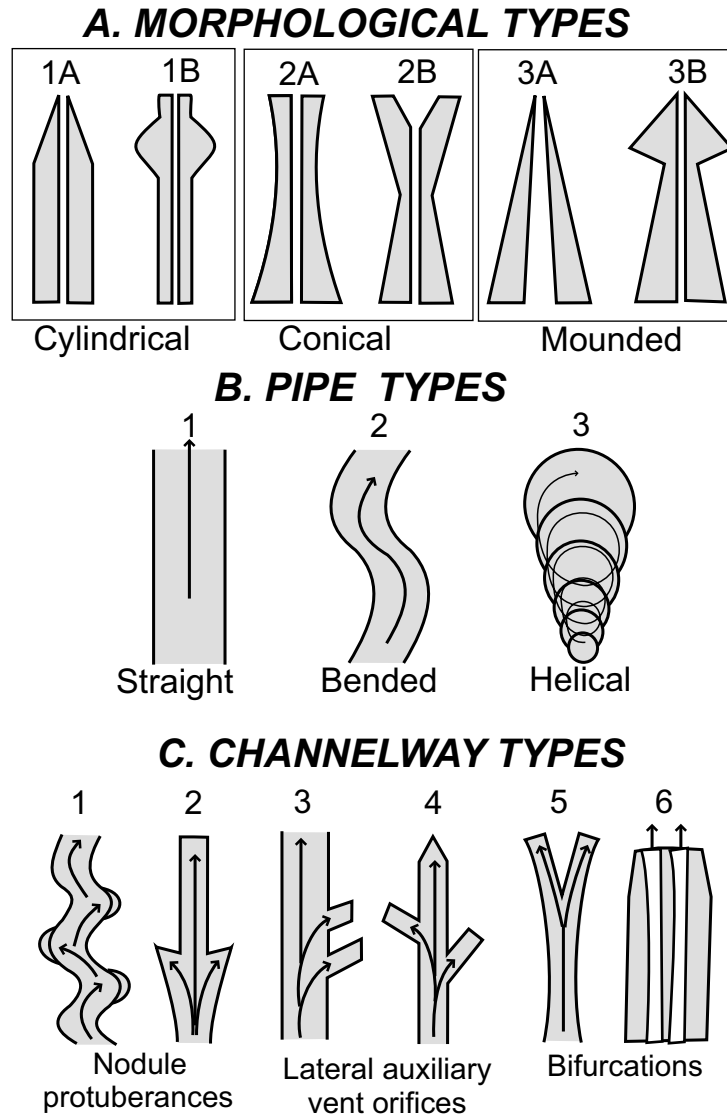


Fig. 6. Simplified sketch of most of the chimney types discovered in the Gulf of Cádiz. (A) Based on their morphologies: Cylindrical pipes (type 1A) with mushroom terminations (type 1B); conical pipes (type 2A) with bifurcations of the vent orifice (type 3B); mound-shaped (type 3A) with mushroom-like termination (type 2B). (B) Pipe types: (1) straight, (2) bent and (3) helical. (C) Channel types: (1) nodule protuberances along the tortuous pipes, (2) nodule protuberances at the base, (3) lateral auxiliary vent orifices on the same side, or (4) at alternating sides, (5) bifurcated vent orifices at the top of main pipe, and (6) chimneys with two vent orifices.

Fig. 5. Photographs of examples of the carbonate chimneys: (A) Helical-type pipe chimney. (B) Conical-type chimney bifurcated into two pipes. (C) Light yellow mounded-type chimney. (D) Three curved bifurcations at the top of a cylindrical pipe-like chimney. (E) Cylindrical pipe-like chimney. (F) Cylindrical pipes with bullet-like termination. (G) Broad cylindrical pipe-like chimney showing protuberances at the base. (H) Characteristic cylindrical pipe-like chimney. (I) Details of the central orifice within a thick cylindrical pipe-like type. (J) Detailed view of the enlarged top of a mounded-type chimney showing the central orifice. (K) Detailed view of a broad central orifice related to thin pipe walls.

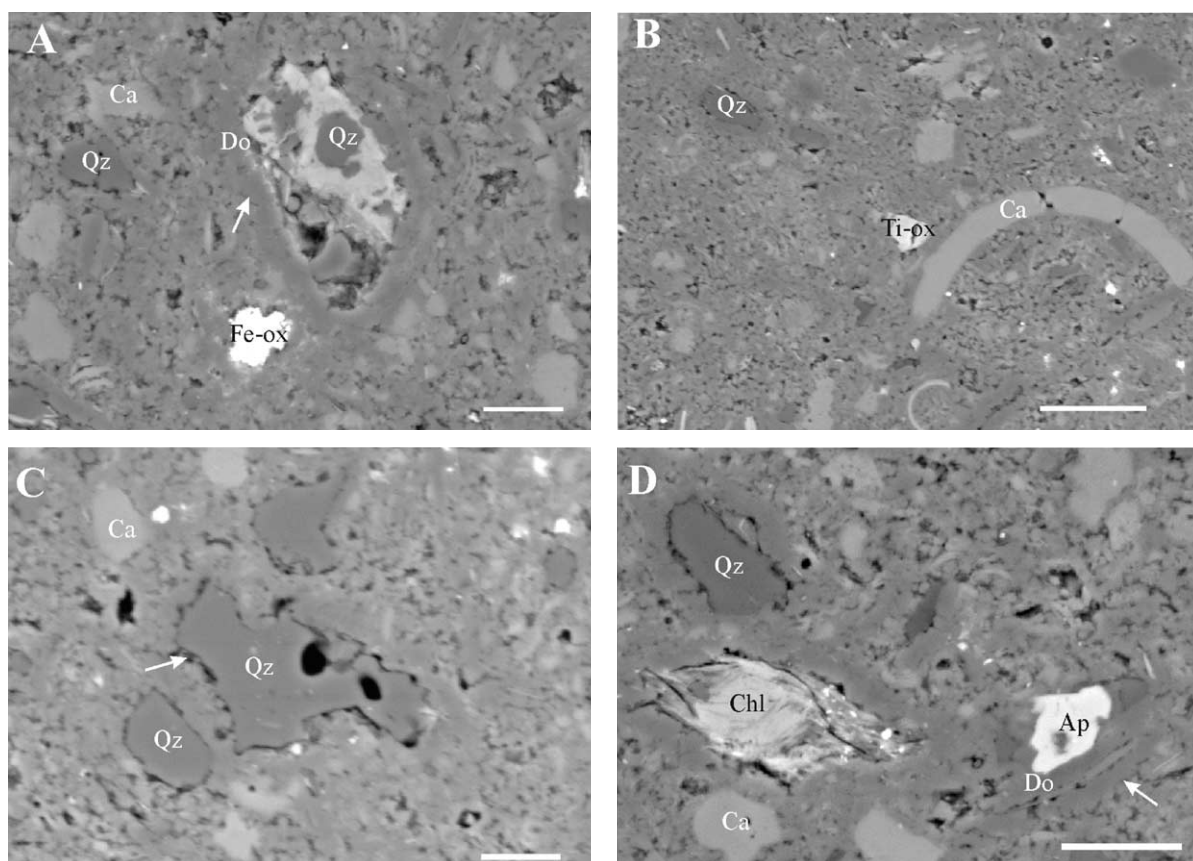


Fig. 7. BSE images of thin sections of chimneys from the Ibérico mound. Fine-grained carbonates can be observed in a porous matrix. Dolomite coatings around detrital grains can be seen in panels A and D (white arrows). Shells and phyllosilicates are also abundant (panels B and D). Quartz grains (panel A, white arrow) show corroded rims. Ca, calcite; Qz, quartz; Do, dolomite; Fe-ox, iron oxides; Ti-ox, titanium oxides; Ap, apatite; and Chl, chlorite. (A,C,D) Scale bar 10 μm . (B) Scale bar 20 μm .

Table 1

Site location and characteristics of the carbonate chimneys from the Gulf of Cádiz

Sample	Field	Site and related structure	Depth (m)	Chimney morphology	Authigenic carbonates (XRD, ^{13}C BSE, OM)	^{18}O	
						(‰ PDB)	(‰ PDB)
ch13	DIASOM	Ibérico mound	870–950	cylindrical	ankerite, calcite, dolomite	–20.81 to –38.36	4.14–5.56
ch25a	DIASOM	Ibérico mound	870–950	small cylindrical	ankerite, dolomite, calcite	–37.64	2.34
ch25b	DIASOM	Ibérico mound	870–950	small cylindrical	ankerite, dolomite, calcite	–21.61	0.71
ch25c	DIASOM	Ibérico mound	870–950	small cylindrical	ankerite, dolomite, calcite	–34.47	2.90
ch77	DIASOM	Ibérico mound	870–950	cylindrical	ankerite, dolomite, calcite	–36.52	3.32
ch24	DIASOM	Ibérico mound	870–950	mounded	dolomite, calcite	–40.02	4.31
ch-h	TASYO	Hespérides mud volcano	750–900	fragment	calcite, dolomite	–23.21	1.93
ch-za	GBF	Salt diapir	500–525	cylindrical	dolomite	–46.25	4.81
ch-zb	GBF	Salt diapir	500–525	cylindrical	dolomite	–46.11	4.82
Ch-mg	ESF	Mud volcano area	450	mushroom-like	dolomite	–37.01	1.31

diameter, which decrease to 13 cm toward the top (Fig. 5C). Vent orifices also decrease in diameter toward the top, with diameters of 6 cm at the base, thinning to 2 cm at the top. Some chimneys attain 55 cm in height and are characterised by a mushroom-like top. Mounded-type chimneys are predominantly light yellow in colour, in contrast to pipe-like and conical types, which are darker brown.

5.3. Mineral chemistry

XRD analysis shows that the most abundant

minerals in the chimneys are carbonates: ankerite, Fe-bearing dolomite, dolomite, and calcite. Table 1 summarises the main carbonate mineralogy of the chimney samples on the basis of XRD data optics, and electron microscopic study (EDS analysis on thin sections). XRD data from six chimneys analysed from the DIASOM field show the main component of the chimneys is ankerite (carbonate with FeO content up to 19.5%) and Fe-bearing dolomite (with FeO content between 12.06 and 19.5%), excepting the mounded-type chimney(ch24), which is formed only by dolomite (with FeO content under 12.05%) as the main

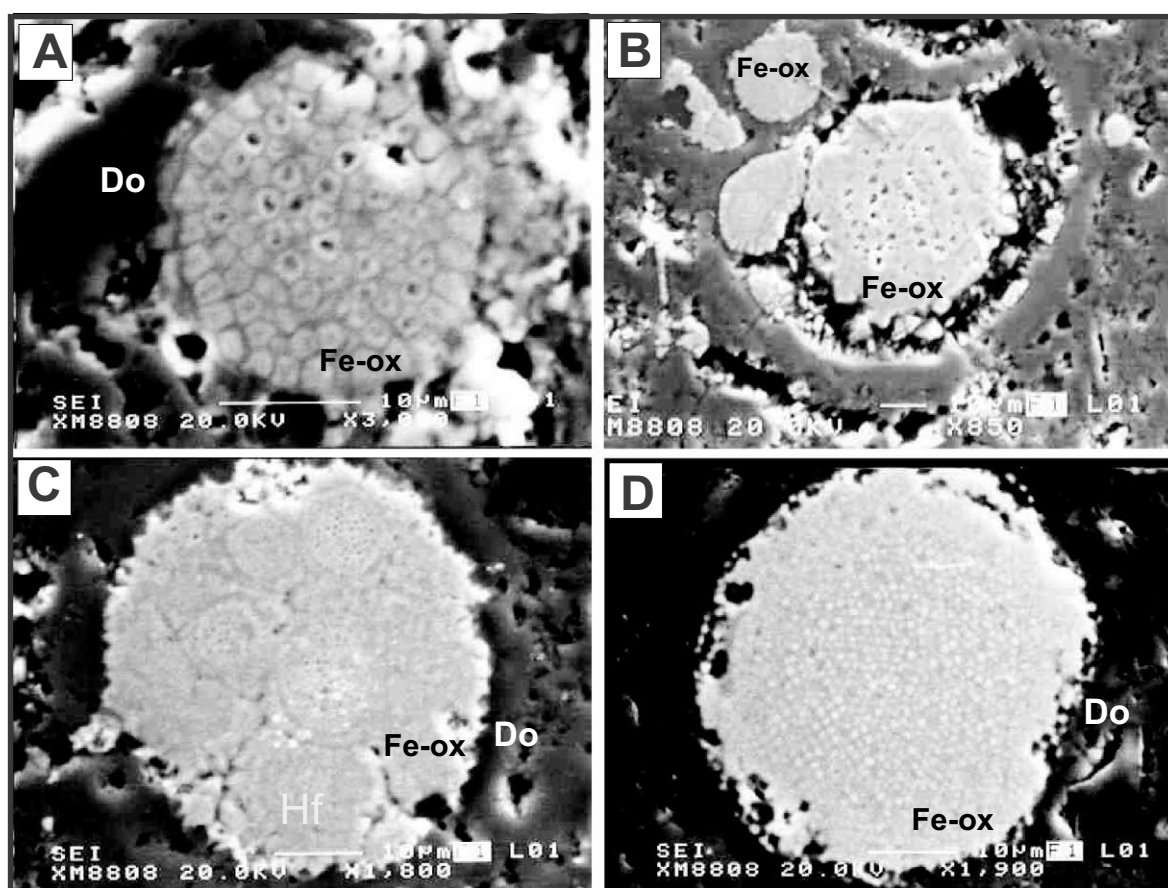


Fig. 8. BSE images of an ankerite chimney (sample ch13) from the Ibérico mound, showing dolomite/iron oxide agglomerates; Fe-ox, iron oxides; Do, dolomite. (A) Pentagonal agglomerate composed of up to 60 single framboids of $\sim 1\text{--}2\ \mu\text{m}$ in size, surrounded by dolomitic micrite. (B) Framboids filling a foraminifera chamber. Note the partial dissolution of the framboid, which is marked by a thin film of iron oxides sealing the internal wall of the foraminifera. (C) Spherical agglomerate composed of 12 complex pentagonal framboids of $\sim 10\text{--}15\ \mu\text{m}$ in size. Note that the overall association is rimmed by dolomitic micrite. (D) Spherical agglomerate composed of single cells, $\sim 0.5\text{--}1\ \mu\text{m}$ in diameter. Note the pitted surface on the boundary with the carbonate rim.

Table 2
Representative elemental chemistry from carbonate chimney samples

Sample	Field	%SiO ₂	%Al ₂ O ₃	%Fe ₂ O ₃	%CaO	%TiO ₂	%MnO	%MgO	%Na ₂ O	%K ₂ O	%P ₂ O ₅	LOI	As	Ba	Co	Cr	Ni	Sc	V	Y
ch13	DIASOM	14.55	2.16	5.393	30.78	0.219	0.072	9.626	0.431	0.561	0.225	35.83	75	94	8	25	17	4	82	8
ch25a	DIASOM	11.4	1.71	10.792	27.83	0.211	0.199	11.263	0.58	0.615	0.713	34.69	60	291	10	37	30	4	129	12
ch25b	DIASOM	9.4	1.59	19.617	29.46	0.24	0.109	6.114	0.512	0.721	0.876	31.36	134	122	20	72	64	7	286	23
ch25c	DIASOM	10.97	1.77	14.071	29.49	0.216	0.087	8.284	0.539	0.657	0.621	33.29	100	112	15	58	48	6	218	21
ch77	DIASOM	10.31	1.41	14.379	26.99	0.218	0.106	11.026	0.485	0.648	0.557	33.87	133	146	17	42	42	5	186	3
ch24	DIASOM	20.55	2.67	3.991	26.86	0.226	0.038	11.074	0.687	0.596	0.265	33.04	37	116	7	39	31	3	62	8
ch-h	TASYO	12.51	1.58	10.744	39.41	0.167	0.089	1.573	0.472	0.411	0.658	32.38	101	193	16	37	42	3	171	10
ch-za	GBF	11.31	1.55	3.397	28.71	0.183	0.047	15.878	0.526	0.652	0.432	37.32	26	625	9	21	12	3	34	5
ch-zb	GBF	11.08	1.61	5.093	27.62	0.168	0.073	15.594	0.566	0.572	0.541	37.08	37	219	7	24	12	4	51	6
ch-mg	ESF	20.25	3.32	2.403	29.10	0.274	0.044	9.552	0.809	0.768	0.186	33.29	20	179	5	37	14	5	44	7

component. Pyrite, iron oxides (goethite and hematite), detrital calcite, quartz, feldspars, phyllosilicates, rutile, zircon, apatite, and monazite have also been detected on the basis of microprobe analyses.

Optical microscopy and backscattered scanning electron (BSE) images of these chimneys (Fig. 7) show that the general texture of the samples is a fossiliferous micrite with abundant forams, worm tubes and silty detrital grains in the carbonated matrix. Authigenic carbonates occur as very fine-grained crystals (micrite) and as crystalline coatings over terrigenous grains (Fig. 7A). The terrigenous components, silt to sand sized, are not in contact with each other and are: quartz, feldspars, phyllosilicates (kaolinite, chlorite and muscovite) and minor oxides (Ti oxides) and phosphates (apatite and monazite) (Fig. 7A–D). Many of the terrigenous components, mainly quartz and feldspar grains, have corroded grains (Fig. 7C) and are armoured or coated with authigenic dolomite (Fig. 7A,D).

BSE images show a wide variety of textures of agglomerates of iron oxide framboids rimmed by dolomite (Fig. 8). Single euhedral framboids show well-faceted pentagonal monocrystals, typical textures of authigenic pyrite (Sweeney and Kaplan, 1973). Associations of single framboids may form different textural types of agglomerates. In this way, single framboids of about 1 µm diameter form pentagonal-shaped agglomerates up to 60 µm in diameter rimmed by dolomite micrite (Fig. 8A). An interfingering boundary is developed between the framboid agglomerate and the surrounding dolomite micrite rim. Some of these framboid agglomerates have been found in the interior of the foraminifera chambers (Fig. 8B). Similar framboidal textures have been suggested as a symbiotic association between foraminifera and chemosynthetic bacteria, providing space for colonisation and local nutrients for bacteria growth (Kohn et al., 1998). Spherical agglomerates are also observed composed of several well-developed pentagonal framboids, up to ~10–15 µm in diameter (Fig. 8C), or by multiple undeveloped single framboids of 0.5–1 µm in diameter (Fig. 8D), rimmed by dolomitic micrite. A characteristic pitted surface is developed at the inter-

shows single cells growing and interfingering at the boundary with the surrounding dolomite micrite rim.

5.4. Geochemical characteristics

Table 2 summarises the major, trace element composition values of the chimneys analysed. If SiO₂ content is taken as a measure of detrital input, the main differences in SiO₂ and Al₂O₃ content can be related to different content of silty-size detrital phases (such as phyllosilicates, feldspars and quartz) in the chimneys. The Fe₂O₃ content is variable, ranging from 3.9 to 19.67%, with the lowest value corresponding to a mounded chimney (that also has 20.55% of SiO₂). In contrast, the chemical and mineralogical composition of the powdery material which fills the central conduits of the chimneys is slightly different

with respect to the composition of the chimneys, showing higher values of SiO₂ (27.09%) and Al₂O₃ (5.97%) and lower values of Fe₂O₃ (2.90%), MgO (1.21%) and As (28 ppm). This material is composed of major quartz and calcite, minor aragonite, and dolomite, muscovite and chlorite as accessory minerals.

A negative relation between the MgO and Fe₂O₃ values is observed in the chimneys of the DIASOM field (Fig. 9A). MgO displays values between 6% and 11.2% whereas the Fe₂O₃ content is highly variable (3.99–19.67%) (Fig. 9A). Samples from cylindrical chimneys with ankerite carbonate show the lowest values of MgO (6%) and higher values of Fe₂O₃ (19.67%). The As, Ni, and Co contents show good correlation with Fe₂O₃ values (Fig. 9B–D). The lowest values of As, Ni, and Co correspond to the mounded-type chimneys and also correspond with the lowest values

Table 3
Isotopic composition from carbonate chimneys

Sample reference	Field	¹³ C (‰ PDB)	¹⁸ O (‰ PDB)	Mineralogy
Biogenic calcite	DIASOM	+0.86	3.36	calcite
ch13-3	DIASOM	−35.98	5.05	ankerite
ch13-4	DIASOM	−37.13	5.56	ankerite
ch13-5	DIASOM	−38.36	5.44	ankerite
ch13-6	DIASOM	−36.73	5.50	ankerite
ch13-7	DIASOM	−33.26	5.18	ankerite
ch13-8	DIASOM	−23.42	4.83	ankerite
ch13-9	DIASOM	−35.77	5.35	ankerite
ch13-10	DIASOM	−33.37	5.00	ankerite
ch13-11	DIASOM	−34.89	5.39	ankerite
ch13-12	DIASOM	−29.88	4.93	ankerite
ch13-13	DIASOM	−20.81	4.14	ankerite
ch13-14	DIASOM	−27.65	4.69	ankerite
ch13-15	DIASOM	−26.38	4.56	ankerite
ch13-16	DIASOM	−24.13	4.36	ankerite
ch13-17	DIASOM	−25.36	4.76	ankerite
ch13-18	DIASOM	−26.43	4.89	ankerite
ch13-19	DIASOM	−33.87	5.05	ankerite
ch13-20	DIASOM	−27.39	4.85	ankerite
ch24	DIASOM	−40.02	4.31	dolomite
ch25a	DIASOM	−37.64	2.34	ankerite, Fe dolomite
ch25b	DIASOM	−21.61	0.71	ankerite, calcite
ch25c	DIASOM	−34.47	2.90	ankerite, calcite
ch77	DIASOM	−36.52	3.32	ankerite, calcite
ch-za	GBF	−46.25	4.81	Fe dolomite
ch-zb	GBF	−46.11	4.82	Fe dolomite
ch-h	TASYO	−23.21	1.93	Calcite/Fe dolomite
ch-mg	ESF	−37.01	1.31	Fe dolomite

of Fe₂O₃, in contrast to the cylindrical chimneys, which show the highest contents of As, Ni, Co, and V. This relation can be partially explained by the relative amount of fine-grained pyrite crystals in these samples, now altered to iron oxides.

5.5. Stable isotopic analyses

Stable carbon and oxygen isotopic analyses from six chimneys from the DIASOM field are summarised in Table 3 and plotted in Fig. 10. Multiple subsamples (20), from the outer and inner walls and at its mushroom-shaped top, were analysed from the ankerite chimney ch13, in order to observe isotopic variability during the formation of the chimneys. In general, the chimneys of the DIASOM field show moderate to low depleted $\delta^{13}\text{C}$ values, varying from -40 to -20‰ and the $\delta^{18}\text{O}$ varies from 0.7 to 5.5‰ . In contrast

to the chimneys, biogenic calcite from coral aggregates shows high $\delta^{13}\text{C}$ values of 0.86‰ and $\delta^{18}\text{O}$ values of 3.36‰ . The lowest values of $\delta^{13}\text{C}$ (as low as -40‰) correspond to the mounded-type chimney (ch24) composed of Fe dolomite. Otherwise, the cylindrical chimneys, composed of ankerite, show moderately depleted $\delta^{13}\text{C}$ values from -37 to -20‰ . This variability is also shown in their $\delta^{18}\text{O}$ values, ranging from 0.71 to 5.6‰ .

Data from multiple subsamples from the chimney (ch13) also show a high variability with moderate depleted $\delta^{13}\text{C}$ values from -38.3 to -20.81‰ , but constant values of the $\delta^{18}\text{O}$ (4.1 – 5.6‰). At the same time, this data sequence shows a relative enrichment in $\delta^{18}\text{O}$ increasing linearly as the $\delta^{13}\text{C}$ values decrease (Fig. 11). Based on the isotopic results and the relative position of the dataset within the same chimney,

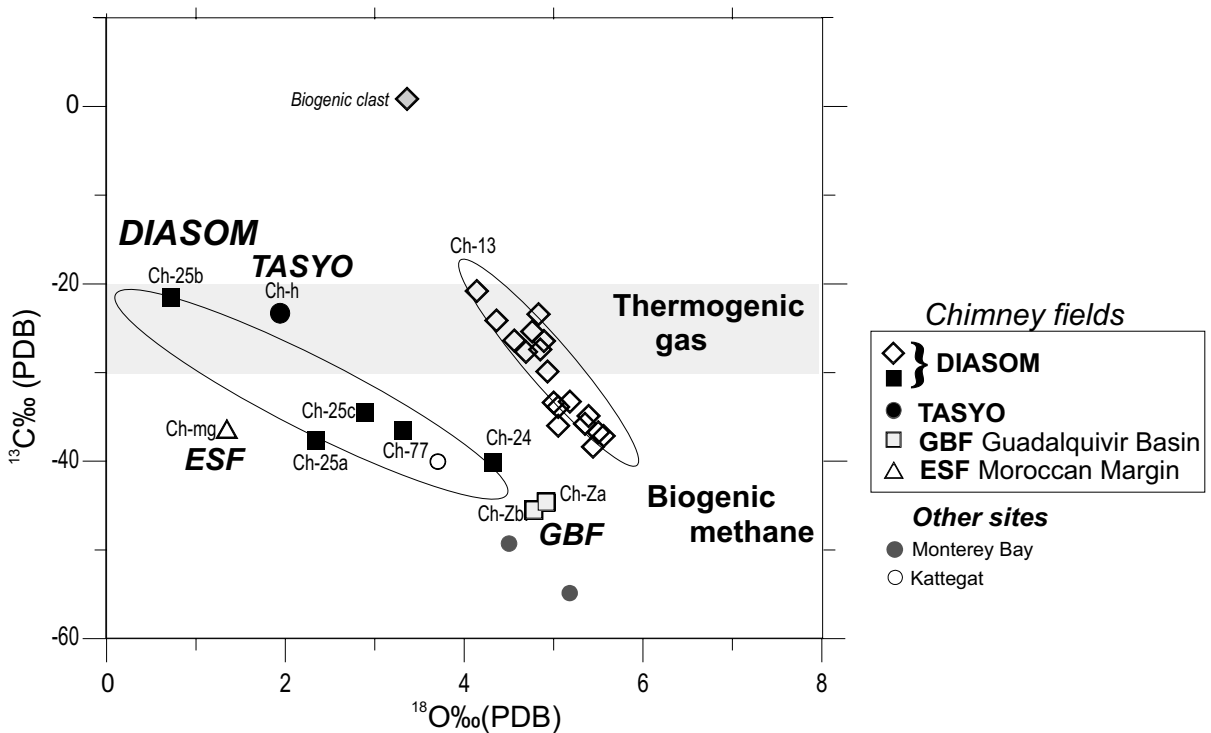


Fig. 10. Plot of $\delta^{13}\text{C}$ and $\delta^{18}\text{O}$ values for carbonate chimney samples from the different fields of the Gulf of Cádiz. See Tables 1 and 3 for an explanation of the sample locations and mineralogy. Isotopic data for representative samples of dolomite chimneys from Monterey Bay (Stakes et al., 1999) and Kattegat (Jørgensen, 1992) have also been plotted. The boundary between thermogenically formed gas and biogenic gas is based on isotopic data of gas-charged sediments in mud volcanoes of the Gulf of Cádiz (Stadnitskaia et al., 2001).

samples can be grouped into three groups. Samples from the inner walls are grouped, showing slightly depleted $\delta^{13}\text{C}$ values from -20 to -26‰ and relatively low $\delta^{18}\text{O}$ values from 4 to 4.75‰ . Conversely, samples from the outer walls show moderately depleted $\delta^{13}\text{C}$ values from -33 to -38‰ and higher values of $\delta^{18}\text{O}$ (up to 5.5‰). On the other hand, samples collected from the mushroom-like structure of the chimney show values of $\delta^{13}\text{C}$ (from -27 to -30‰) and $\delta^{18}\text{O}$ (4.75 – 55.5‰), intermediate between the values characteristic of the inner and outer walls. This variability of the isotopic data within the same chimney points out the existence of changes in the sources of the hydrocarbon fluid venting, formation temperature and/or pore fluid isotopic

composition during the formation of the chimneys.

6. Discussion

6.1. Hydrocarbon flux rates and carbonate chimney setting

The formation of carbonate chimneys and other features originating from such mineralisation (e.g. carbonate mounds, nodules) are related to slow flux rates of fluids and gases released to the sea floor in the Gulf of Mexico (Carney, 1994; Roberts, 2001). Ankerite and dolomite authigenic carbonates are typically associated with

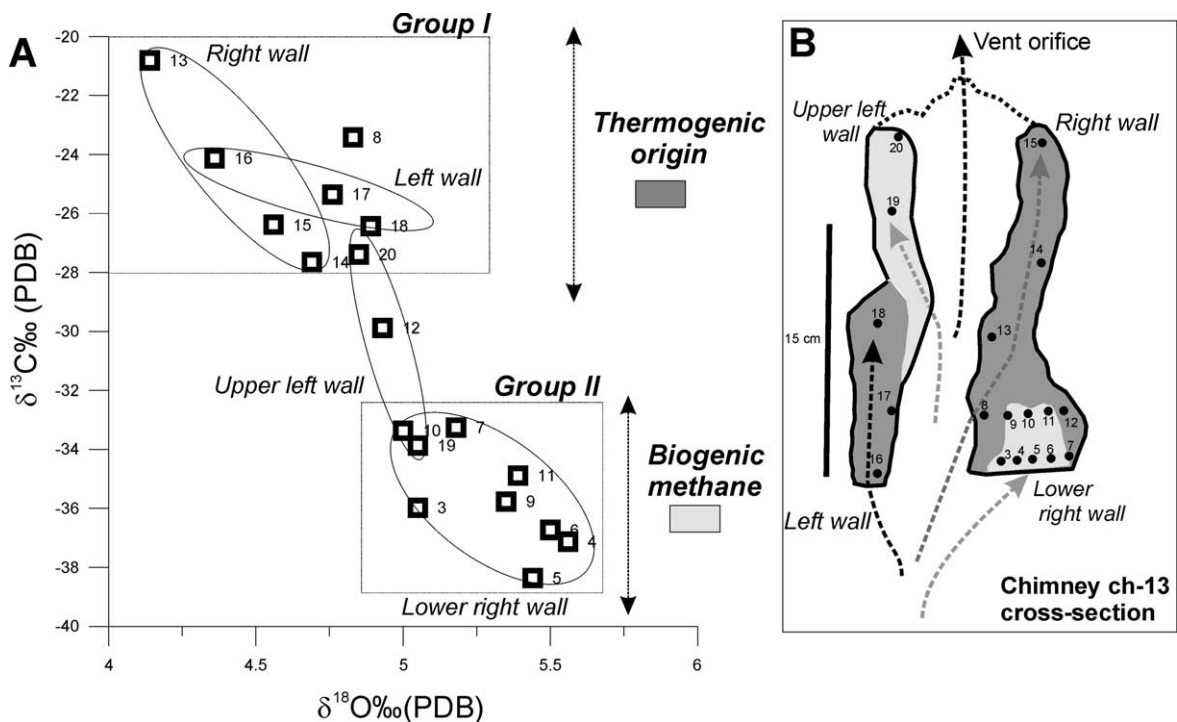


Fig. 11. (A) Plot of $\delta^{13}\text{C}$ and $\delta^{18}\text{O}$ values for the ankerite chimney ch13 from the Ibérico mound: Group I shows low depleted $\delta^{13}\text{C}$ values (-20 to -26‰) and low $\delta^{18}\text{O}$ values interpreted as derived from thermogenic sources or high-order hydrocarbon. Group II shows more depleted $\delta^{13}\text{C}$ values from -33 to -38‰ that fit better within the isotopic window for biogenic gas in the Gulf of Cádiz (Stadnitskaia et al., 2001). (B) Sketch of the cross section of the ankerite chimney ch13, from the Ibérico mound, showing the positions of subsamples used for the $\delta^{13}\text{C}$ isotopic determinations. Darker grey areas represent walls with isotopic values from Group I; light grey areas show walls with isotopic data from Group II. Blanking inside shows the main vent conduit. Arrows suggest a model of accretion for the chimney walls, built up by distinct and alternating periods of thermogenically and biogenic-derived fluid venting. See text for more detailed explanation.

pore fluids below the zone of sulphate reduction, representing the deepest formation zone with suitable thermal conditions, as in the Blake Ridge (Greinert et al., 2001). In this way, all of the chimney-like carbonate structures described for the west coast of the US have been unanimously interpreted as subsurface structures as a result of methane venting from deeper levels of microbial methanogenesis and may include fluids that had been sequestered as a clathrate (Stakes et al., 1999). The few examples of authigenic carbonates that formed at the sediment water interface tend to be dominated by aragonite mineralogies, where high sulphate concentrations inhibit precipitation of high-Mg calcite and dolomite (e.g. Hydrate Ridge, Greinert et al., 2001). At the same time, the variability in the carbonate-type phase of chimney-like structures has also been related to the rate of venting in the Kattegat (Jørgensen, 1992), where large fluxes of methane produce dolomite cementation, whereas high-Mg calcite and aragonite precipitate when fluxes are lower.

The mechanism assumed for the formation of the dolomite chimneys is the slow flux of channelised fluids and gases released to the sea floor, probably through fault planes, from subsurface levels of bacterially induced fermentation (Stakes et al., 1999). Following the criteria of formation of dolomite chimneys and authigenic siderites reported in other cold seeps (e.g. Blake Ridge, Monterey Bay, Kattegat), this type of chimneys would have cement pipes as a result of subsurface fluid flow and mineral deposition under the sea floor rather than at the water interface. The Blake Ridge siderites, in fact, were only present several hundred metres below the zone of hydrate stability. Strong erosional processes and remobilisation of the host sediments might explain their present location on the sea floor. It is not clear, however, whether such strong erosional processes occur in the sites studied in the Gulf of Cádiz, nor whether all the chimneys result from a similar process. The fact that underwater observations show a high density of chimneys overlying the sea floor in most of the sites and, in addition, mushroom-like chimneys protruding from muddy patches, could indicate that some types could also form at the water–sediment interface.

6.2. Geochemical variations and the role of bacterial anaerobic oxidation of methane (AOM)

The chimneys collected in the Gulf of Cádiz mainly consist of three different types of authigenic carbonates: ankerite, Fe-bearing dolomite and calcite. The Fe_2O_3 contents of the bulk samples display a high variability, ranging from 2.40% to 19.61%, and could be moderately negatively correlated with MgO contents, from 6.11 to 11.26% (Fig. 9A). Chimneys from the DIASOM field show the largest content of Fe_2O_3 and are formed by ankerite and Fe dolomite. The cylindrical chimneys in this field show the highest values of Fe_2O_3 (up to 20%) whereas mounded-type chimneys show low values (lower than 4%). The mushroom-like chimney of the Moroccan margin (ESF field) shows the lowest content in Fe_2O_3 (lower than 2.5%). The highest values of MgO (higher than 15%) and low values of Fe_2O_3 (lower than 4%) are shown in a dolomite chimney of the GBF which is also associated with salt diapirism. This chimney also shows high values of Ba (600 ppm), related to the presence of barite. Otherwise, samples of chimneys from mud volcanoes of the TASYO field, composed mainly of calcite and Fe dolomite, show intermediate values of iron oxides (10%) and low values of MgO (lower than 2%).

The content of Fe_2O_3 shows a strong positive correlation with As, Co, Ni in all chimneys sampled in the Gulf of Cádiz (Fig. 9). There seems to be an overall relation between Fe and Mg cations and the production of biogenic pyrite, oxidised to iron oxides. One possible scenario is the formation of the dolomite/iron oxide agglomerates, which could be related to bacterial AOM, a process fundamental to the nourishment of the chemosynthetic cold seep communities and involving formation of authigenic carbonates from hydrocarbon seeps (Hovland et al., 1987). Symbiotic cooperation between the consortium of archaea and sulphate reducing bacteria (SRB) (Boettius et al., 2000) is the mechanism claimed to explain the biomineralisation and abundance of this type of agglomerate. On the basis of the agglomerate textures and geochemical relationships, we suggest that the consortium between methane-oxidising archaea and SRB could be responsible

for this type of biomineralisation (Fig. 8). In this way, pyrite framboids are the product of SRB (Belenkai, 2000), whereas the surrounding archaea may be responsible for the dolomite micrite rims as products of AOM. This is supported by the fact that new data on cold seeps show that these archaea can also occur as single cells or in clumps (Boetius, 2002). The relationship between bacterial activity and biomineralisation is also supported by the presence of similar pyrite within the gills of living mussels (Streams and Fisher, 1997) and within foraminifera chambers (Kohn et al., 1998). What is not clear at present is the nature of the micro-organisms involved in the formation of the chimneys, and the influence of micro-organism activity on dissolved carbonate equilibria and carbonate mineralogy is poorly understood.

6.3. Carbon isotopic variations: biogenic vs thermogenic origin

Authigenic carbonates inherit the $\delta^{13}\text{C}$ values characteristic of their specific carbon sources and even though some mixing is expected, the $\delta^{13}\text{C}$ signature is an indication of the microbial processes in vent-related carbonate deposits (Aharon et al., 1992). The $\delta^{13}\text{C}$ values for authigenic carbonates in the Gulf of Mexico from areas seeping primarily crude oil have $\delta^{13}\text{C}$ values that are close to the crude oil range of values (-25% to -35% PDB). Similar carbonates from methane seeps are more $\delta^{13}\text{C}$ -depleted (Roberts and Aharon, 1994) and in those from gas hydrate areas, the $\delta^{13}\text{C}$ values range between -40% and -55% (Sassen et al., 1999). In the Gulf of Cádiz, carbon isotopic data from C2–C5 hydrocarbon gases measured on mud volcanoes are moderately depleted $\delta^{13}\text{C}$ values (-19.2% to -29%) whereas biogenic methane values display extremely depleted $\delta^{13}\text{C}$ values ranging from -32% to -63% (Stadnitskaia et al., 2001).

In this sense the $\delta^{13}\text{C}$ values from the ankerite chimneys of the DIASOM field, ranging from -20.81% to -35% , fall almost entirely within the window of thermogenically formed gas (Fig. 10). In contrast, only the mounded-type chimney (ch24) shows extreme $\delta^{13}\text{C}$ depletion, with values

of -40% , indicating their probable origin from a biogenic methane source. Furthermore, the dataset of $\delta^{13}\text{C}$ values within chimney ch13 points to the existence of some types of variability in the hydrocarbon sources of the fluid venting, from thermogenic to biogenic, during the formation of the chimneys in this field (Fig. 11A). Two main groups are identified based on isotopic data: Group I, showing low depleted $\delta^{13}\text{C}$ values (-20 to -26% PDB) and low $\delta^{18}\text{O}$ values, interpreted as derived from thermogenic or high-order hydrocarbon sources (Roberts and Aharon, 1994); and Group II, showing more depleted $\delta^{13}\text{C}$ values from -33 to -38% that fit better within the isotopic window for biogenic gas in the Gulf of Cádiz (Stadnitskaia et al., 2001). The fact that these two groups are arranged in different walls or parts of the chimneys (Fig. 11B) suggests a model of accretion in which a chimney builds up by alternating periods of thermogenic and biogenic-derived fluid venting more than as a mixing process of different hydrocarbon sources.

The $\delta^{13}\text{C}$ values from the calcite chimney collected in the Hespérides mud volcano and associated with a mud diapir (Somoza et al., this volume) located in the TASYO field, also show values of -23.2% , possibly related to a thermogenic gas source (Fig. 10). In contrast, on the Moroccan margin, in the ESF field, isotopic values of -37% , corresponding to Fe-bearing dolomite chimneys with mushroom morphology, indicate their possible origin as mixing between thermogenic and biogenic sources. The most extremely $\delta^{13}\text{C}$ -depleted values obtained in the Gulf of Cádiz correspond to the chimney analysed from the GBF field, associated with salt diapirism and also with the presence of the barite (Ba values up to 600 ppm in Table 2). Extremely depleted $\delta^{13}\text{C}$ values of -46% indicate their possible source as entirely from methane release (Fig. 10).

6.4. Oxygen isotope variations: temperatures of formation

The relationship between isotopic fractionation of oxygen and temperature, in the carbonate–water system, indicates that the dolomites of the chimneys are formed between 8.7 and 13.9°C.

Formation temperatures are calculated using the equation for the siderite–water system and assuming a $\delta^{18}\text{O}$ for seawater of 0‰ (Standard Mean Ocean Water, SMOW). The palaeotemperatures are consistent with modern bottom water temperatures, varying from 10 to 13°C in all fields sampled (Gardner et al., 2001).

The isotopic data sequence from chimneys in the Gulf of Cádiz shows relative enrichment in $\delta^{18}\text{O}$, with $\delta^{18}\text{O}$ values increasing linearly as the $\delta^{13}\text{C}$ values decrease (Fig. 10). This linear relationship is clearly observed in datasets from chimney ch13 (Fig. 11), which shows a high variability in $\delta^{18}\text{O}$ from 4 to 5.6‰ PDB. The enrichment in $\delta^{18}\text{O}$ has been explained in other areas of cold seeps, as the expulsion of free gas from subsurface clathrate formations (Sakai et al., 1992; Hackworth and Aharon, 2000). Gas hydrate decomposition affects the oxygen isotope composition due to the release of ^{18}O -enriched waters (Davidson et al., 1983). The role of dissociation of gas hydrate, yielding a net production of CO_2 depleted in $\delta^{13}\text{C}$ and enriched in $\delta^{18}\text{O}$ (Sassen et al., 1999), in the formation of these chimneys, is a phenomenon still poorly understood. The gas released from the hydrates collected on the Moroccan margin of the Gulf of Cádiz is essentially hydrocarbonic with a high content of methane homologues, indicating its thermogenic nature and suggesting the existence of hydrocarbons and gas-rich overpressured sediments at depth, and the upward migration of these fluids and fluidised sediments along faults to the sea floor (Stadnitskaia et al., 2000). Bottom water temperatures of 12.1°C and geothermal gradients of 23.68°C/100 m result in a thickness of the hydrate stability zone (HSZ) of 125 m for the DIASOM field (Gardner et al., 2001). Based on these data, we suggest that the sequestering of upward-flowing gases by subsurface clathrates and the episodic warming by the Mediterranean outflow could be an additional mechanism for the formation of the chimneys in the Gulf of Cádiz (Somoza, 2001).

7. Summary and conclusions

In this paper we report the first discovery and

sampling of hydrocarbon-derived carbonate chimneys in the Gulf of Cádiz. Carbonate chimneys have been found in four different areas, named the DIASOM, TASYO, GBF (Guadalquivir Basin) and ESF (East Moroccan) fields. The chimneys collected (up to 200 samples) show an unusually wide range of sizes and morphologies in comparison with other areas with extensive cold seeps. Chimney tubes can be straight, tortuous, ramified, and of helical type, showing complex internal structures with tortuous fluid channels, nodule protuberances, and auxiliary vent orifices. The underwater camera shows a spectacular density of chimneys overlying the sea floor, and some small mushroom-like pipes protruding from muddy patches. Coring on these host sediments yielded indications of gas saturation, such as degassing structures and a H_2S smell. Local fissures and alignment of isolated chimneys were also observed, suggesting their distribution controlled by fault planes.

Chimneys from all of these fields show similar petrographic characteristics, being mainly formed by authigenic carbonates in different phases with distinctive contents of Fe–Mg (ankerite, Fe-bearing dolomite and calcite), framboidal agglomerates of iron oxides and detrital calcite, quartz and phyllosilicates. Authigenic carbonates occur as micrites and coatings around detrital grains and framboidal agglomerates. The Fe_2O_3 percentages show a strong positive correlation with As, Co, and Ni contents in all chimneys sampled in the Gulf of Cádiz, indicating a relationship between Fe content and microbiological production. We suggest that the abundance of textural types of dolomite/iron oxide agglomerates might be associated with consortia of AOM aggregates involving both production of framboids by SRB and dolomite micrite by methane-oxidising microorganisms, which generally include archaea. Detailed petrographic and microbiological studies of these vast fields of chimneys are currently underway.

$\delta^{13}\text{C}$ isotopic data show significant differences, which may be related to distinct sources of hydrocarbon fluid venting within the Gulf of Cádiz. In this sense, the $\delta^{13}\text{C}$ values from the ankerite chimneys of the DIASOM field fall almost entirely within the window of thermogenically formed

gas (–20 to –32‰), whereas the mounded-type chimneys (Fe-bearing dolomite and calcite) in the same fields show extreme $\delta^{13}\text{C}$ -depleted values (–40‰), related to biogenic methane sources. Moreover, the dataset of $\delta^{13}\text{C}$ values from the outer and the inner chimney walls suggests that the formation of the chimneys in this field is caused by alternating fluid venting from thermogenic and biogenic sources rather than through a process of mixing different hydrocarbon sources.

The $\delta^{13}\text{C}$ data from calcite chimneys collected on the Hespérides mud volcano and associated with mud diapirism (TASYO field) show low values of –23.2‰, possibly related to a thermogenic gas source. In contrast, Fe-bearing dolomite chimneys in the Moroccan margin, the ESF field, indicate their possible origin as mixing between thermogenic and biogenic sources. The most extremely $\delta^{13}\text{C}$ -depleted values obtained in the Gulf of Cádiz are from the chimney analysed from the GBF field, associated with salt diapirism and with the characteristic presence of barite. These extremely depleted $\delta^{13}\text{C}$ values of –46‰ indicate their possible source as entirely from methane release.

These considerations suggest that the structure and nature of these pipe-like carbonate chimneys in the Gulf of Cádiz are related to channelised and slow flux of fluids and gases released to the sea floor through fault planes from subsurface levels of bacterially induced fermentation. Therefore, the formation of these vast fields of carbonate chimneys implies new considerations on the importance of hydrocarbon fluid venting in this area and, moreover, on the active role of the olistostrome/accretionary wedge of the Gibraltar arc, the westernmost compressional Mediterranean arc under the compressional stress of the Eurasian and African plates. Otherwise, the role of episodic dissociation of gas hydrate, yielding a net production of CO_2 depleted in $\delta^{13}\text{C}$ and enriched in $\delta^{18}\text{O}$ in the formation of these chimneys, is a process still poorly understood. In this sense, the sequestering of upward flows of gases by subsurface clathrates, and the episodic warming by the Mediterranean outflow waters, could be an additional mechanism for the formation of the chimneys in the Gulf of Cádiz.

Acknowledgements

This paper is dedicated to the memory of Jesus Baraza, our colleague. This research was funded by the Spanish Marine Science and Technology Program, under the TASYO Project No. 98-0209, in the framework of the Spanish–Portuguese agreement for scientific cooperation. The authors thank all those who participated in the research cruises of the TASYO project, specially the captains and crews of both the R/V *Cornide de Saavedra* and the R/V *Hespérides* for their expertise in collecting the samples. In addition, special appreciation is expressed to Francisco Sanchez for his role in the acquisition of the underwater images and to Ana Lobato and Jesús Rodero for their help in processing of the multibeam data. We are grateful to the Electronic Microscopy Laboratory of the Universidad Complutense de Madrid for providing help in microprobe and scanning microscopy. Debra Staker and Silke Severmann greatly improved this manuscript with thoughtful and thorough reviews. We thank John Woodside for his valuable input. Also, we gratefully acknowledge informal discussions on microbial-related processes with Martin Hovland, Antje Boetius and Marina Cunha. We are especially grateful to Michael Ivanov and Luis Pinheiro for their helpful cooperation in the framework of the TTR IOC-UNESCO Program.

References

- Aharon, P., Graber, E.R., Roberts, H.H., 1992. Dissolved carbon and $\delta^{13}\text{C}$ anomalies in the water column caused by hydrocarbon seep on the northwestern Gulf of Mexico slope. *Geo-Mar. Lett.* 12, 33–40.
- Baoshum, F., Aharon, P., Byerly, G.R., Roberts, H.H., 1994. Barite chimneys in the Gulf of Mexico slope: Initial report on their petrography and geochemistry. *Geo-Mar. Lett.* 12, 81–87.
- Baraza, J., Ercilla, G., 1996. Gas-charged sediments and large pockmark like features on the Gulf of Cadiz slope (SW Spain). *Mar. Petr. Geol.* 13, 253–261.
- Belenkaia, I., 2000. Gas-derived carbonates: Reviews in morphology, mineralogy, chemistry and isotopes (data collected during the TTR Programme cruises during 1995–1999). *Final Proc. VI Int. Conf. Gas in Marine Sediments*, St. Petersburg, Russia, pp. 9–10.

- Berástegui, X., Banks, C.J., Puig, C., Taberner, C., Waltham, D., Fernández, M., 1998. Lateral diapiric emplacement of Triassic evaporites at the southern margin of the Guadalquivir Basin, Spain. In: Mascle, A., Puigdefábregas, C., Luterbacher, H., Fernandez, M. (Eds.), *Cenozoic Foreland Basins of Western Europe*. Geol. Soc. Spec. Publ. 134, pp. 49–68.
- Blankenship, C.L., 1992. Structure and paleogeography of the External Betic Cordillera, southern Spain. *Mar. Petr. Geol.* 9, 256–264.
- Boetius, A., 2002. Anaerobic oxidation of methane mediated by microbial consortium in gassy sediments. Final Proc. Int. Conf. Fluid Escape Structures and Tectonics at Continental Margins and Ocean Ridges, Aveiro, Portugal, p. 67.
- Boetius, A., Ravensschlag, K., Schubert, C., Rickert, D., Widdel, F., Gieseke, A., Amann, R., Jørgensen, B.B., Witte, U., Pfannkuche, O., 2000. A marine microbial consortium apparently mediating anaerobic oxidation of methane. *Nature* 407, 623–626.
- Camoin, G.F., 1999 (Ed.). *Microbial Mediation in Carbonate Diagenesis*. Spec. Issue Sediment. Geol. 126. Elsevier, Amsterdam.
- Carney, R.S., 1994. Consideration of the oasis analogy for chemosynthetic communities at Gulf of Mexico hydrocarbon vents. *Geo-Mar. Lett.* 14, 149–159.
- Cunha, M.R., Subida, M.D., Vandendriessche, S., Lima, I., Ravara, A., and the TTR 11 scientific party, 2002. Macrofaunal communities associated to the carbonate chimneys from the Gulf of Cádiz. Preliminary results from the video imagery and dredge sampling obtained during the TTR-11 Cruise. Final Proc. Int. Conf. Fluid Escape Structures and Tectonics at Continental Margins and Ocean Ridges, Aveiro, Portugal, pp. 77–78.
- Davidson, D.W., Leaist, D.G., Hesse, R., 1983. Oxygen-18 enrichment in the water of a clathrate hydrate. *Geochim. Cosmochim. Acta* 32, 415–432.
- Díaz-del-Río, V., Somoza, L., Martínez-Frias, J., Hernandez-Molina, F.J., Lunar, R., Fernandez-Puga, M.C., Maestro A., Terrinha, P., Llave, E., Garcia, A., Garcia, A.C., Vazquez, J.T., 2001. Carbonate chimneys in the Gulf of Cadiz: Initial report of their petrography and geochemistry. Final Proc. Int. Conf. Geological Processes on Deep-Water European Margins, Moscow, Russia. UNESCO IOC Workshop Report 175, pp. 53–54.
- Fernández-Puga, M.C. Somoza, L., Lowrie, A., Maestro, A., León, R., Díaz del Río, V., 2000. Fluid seeps associated with gravity spreading of salt/shale along the Gulf of Cádiz continental slope. Final Proc. Int. Conf. Geological Processes on European Continental Margins, Granada, Spain. UNESCO IOC Workshop Report 168, pp. 21–22.
- Flinch, J.A., Bally, A.W., Wu, S., 1996. Emplacement of a passive margin evaporitic allochthon in the Betic Cordillera of Spain. *Geology* 24, 67–70.
- Gardner, J.M., 2001. Mud volcanoes revealed and sampled on the western Moroccan continental margin. *Geophys. Res. Lett.* 28, 334–342.
- Gardner, J.M., Vogt, P.R., Somoza, L., 2001. The possible effect of the Mediterranean Outflow Water (MOW) on gas hydrate dissociation in the Gulf of Cádiz. EOS Trans. AGU 82 (47), Fall. Meet. Suppl. Abstracts OS12B-0418.
- Greinert, J., Bohrmann G., Suess, E., 2001. Gas hydrate-associated carbonates and methane-venting at Hydrate Ridge: Classification, distribution and origin of authigenic lithologies. In: Paull, C.K., Dillon, W.K. (Eds.), *Natural Gas Hydrates: Occurrence, Distribution and Detection*. AGU Geophys. Monogr. 124, pp. 99–113.
- Hackworth, M., Aharon, P., 2000. Authigenic carbonate precipitation driven by episodic gas hydrate sublimation: evidence from the Gulf of Mexico. Final Proc. 6th Int. Conf. on Gas in Marine Sediments, St. Petersburg, Russia, pp. 46–47.
- Hovland, M., Talbot, M.R., Qvale, H., Olausen, S., Aasberg, L., 1987. Methane-related carbonate cements in pockmarks of the North Sea. *J. Sediment. Petrol.* 57, 881–892.
- Hovland, M., Judd, A.G. 1988. Seabed Pockmarks and Seepages. Impact on Geology, Biology and the Marine Environment. Graham and Trotman, London.
- Ivanov, M.K., Kenyon, N., Nielsen, T., Wheeler, A., Monteiro, J., Gardner, J., Comas, M., Akhmanov, G., Akhmetzhanov, A., Scientific Party of the TTR-9 cruise, 2000. Goals and principal results of the TTR-9 cruise. Final Proc. Int. Conf. Geological Processes on European Continental Margins, Granada, Spain. UNESCO IOC Workshop Report 168, pp. 3–4.
- Jørgensen, N.O., 1992. Methane-derived carbonate cementation of marine sediments from the Kattegat, Denmark: Geochemical and geological evidence. *Mar. Geol.* 103, 1–13.
- Kohn, M.J., Riciputi, L.R., Stakes, D., Orange, D.L., 1998. Sulfur isotope variability in biogenic pyrite: reflections of heterogeneous bacterial colonization? *Am. Mineral.* 83, 1454–1468.
- León, R., Somoza, L., Ivanov, M.K., Díaz-del-Río, V., Lobato, A., Hernandez-Molina, F.J., Fernandez-Puga, M.C., Maestro, A., Medialdea, T., Alveirinho, J., Vazquez, T., 2001. Seabed morphology and gas venting in the Gulf of Cadiz mud volcano area: Imagery of multibeam data and ultra-high resolution data. Final Proc. Int. Conf. Geological Processes on Deep-Water European Margins, Moscow, Russia. UNESCO IOC Workshop Report 175, pp. 43–45.
- Lowrie, A., Hamiter, R., Moffett, S., Somoza, L., Maestro, A., Lerche, I., 1999. Potential pressure compartments sub-salt in the Gulf of Mexico and beneath massive debris flows in the Gulf of Cadiz. Final Proc. 19th Conf. GCSSEPM Advanced Reservoir Characterization, Houston, TX, USA, pp. 271–280.
- Maldonado, A., Somoza, L., Pallares, L., 1999. The Betic orogen and the Iberian-African boundary in the Gulf of Cádiz: geological evolution (central North Atlantic). *Mar. Geol.* 155, 9–43.
- Orange, D.L., Greene, H.G., Reed, D., Martin, J.B., McHugh, C.M., Ryan, W.B.F., Maher, N., Stakes, D.S., Barry, J., 1999. Widespread fluid expulsion on a translational continental margin; mud volcanoes, fault zones, headless canyons, and organic-rich substrate in Monterey Bay, California. *Geol. Soc. Am. Bull.* 111, 992–1009.

- Orpin, A.R., 1997. Dolomite chimneys as possible evidence of coastal fluid expulsion, uppermost Otago continental slope, southern New Zealand. *Mar. Geol.* 138, 251–267.
- Perconig, E., 1960–62. Sur la constitution géologique de l'Andalouse Occidentale, en particulier du bassin du Guadalquivir (Espagne Méridionale). In: *Livre Mémoire du Professeur Paul Fallot. Mémoires hors-Série de la Société géologique de France*, pp. 229–256.
- Roberts, H.H., 2001. Fluid and gas expulsion on the Northern Gulf of Mexico Continental Slope: Mud-prone to mineral-prone responses. In: Paull, C.K., Dillon, W.K. (Eds.), *Natural Gas Hydrates: Occurrence, Distribution and Detection*. AGU Geophys. Monogr. 124, pp. 145–161.
- Roberts, H.H., Aharon, P., 1994. Hydrocarbon derived carbonate buildups of the northern Gulf of Mexico continental slope: A review of submersible investigations. *Geo-Mar. Lett.* 14, 135–198.
- Roberts, H.H., Carney, R.S., 1997. Evidence of episodic fluid, gas and sediment venting on the Northern Gulf of Mexico Continental Slope. *Econ. Geol.* 92, 863–879.
- Sakai, H., Gamo, T., Ogawa, Y., Boluegue, J., 1992. Stable isotopic ratios and origins of carbonates associated with cold seepage at the eastern Nankai Trough. *Earth Planet. Sci. Lett.* 109, 391–404.
- Sassen, R., Joye, S., Sweet, S.T., DeFreitas, D.A., Milkov, A.V., MacDonald, I.R., 1999. Thermogenic gas hydrates and hydrocarbon gases in complex chemosynthetic communities, Gulf of Mexico continental slope. *Org. Geochem.* 30, 485–497.
- Schroeder, N., Kulm, L.D., Muehlberg, G.E., 1987. Carbonate chimneys on the outer continental shelf; evidence for fluid venting on the Oregon margin. *Oregon Geol.* 49, 91–96.
- Somoza, L., 2001. Hydrocarbon seeps, gas hydrates, and carbonate chimneys in the Gulf of Cadiz: an example of the interaction between tectonic and oceanographic controlling factors. In: Van der Meer, F., Scholte, K. (Eds.), *Natural Hydrocarbon Seeps, Global Tectonics and Greenhouse Gas Emissions*. ESF-LESF Workshop, Delft, The Netherlands, p. 18.
- Somoza, L., Díaz del Río, V., Hernández-Molina, F.J., León, R., Lobato, A., Alveirinho, J.M., Rodero, J., 2000. New discovery of a mud-volcano field related to gas venting in the Gulf of Cádiz: Imagery of multibeam data and ultra-high resolution data. *Final Proc. 3rd Int. Symp. Iberian Atlantic Continental Margin*. Faro, Portugal, pp. 397–398.
- Somoza, L., Díaz-del-Río, V., León, R., Ivanov, M., Fernández-Puga, M.C., Lobato, A., Maestro, A., Hernández-Molina, F.J., Gardner, J.M., Rodero, J., Pinheiro, L.M., Vázquez, J.T., Medialdea, T., Fernández-Salas, L.M., 2003. Seabed morphology and hydrocarbon seepage in the Gulf of Cádiz mud-volcano area: Imagery of multibeam data and ultra-high resolution data. *Mar. Geol.*, S0025-3227(02)00686-2.
- Somoza, L., Ivanov, M.K., Pinheiro, L., Maestro, A., Lowrie, A., Vázquez, J.T., Gardner, J., Medialdea, T., Fernández-Puga, M.C., 2001. Structural and tectonic control of fluid seeps and mud volcanoes in the Gulf of Cadiz. *Final Proc. Int. Conf. Geological Processes on Deep-Water European Margins*, Moscow, Russia. UNESCO IOC Workshop Report 175, pp. 41–42.
- Somoza, L., Maestro, A., Lowrie, A., 1999. Allochthonous blocks as hydrocarbon traps in the Gulf of Cádiz. *Final Proc. Offshore Technology Conf.*, Houston, TX, USA, pp. 571–577.
- Stadnitskaia, A., Ivanov, M., Gardner, J., 2000. Hydrocarbon gas distribution in mud volcanic deposits of the Gulf of Cadiz. Preliminary results. *Final Proc. Int. Conf. Geological Processes on European Continental Margins*, Granada, Spain. UNESCO IOC Workshop Report 168, p. 17.
- Stadnitskaia, A., Ivanov, M., van Weering, T.C.E., Sinnighe Damsté, J.S., Werne, J.P., Kreulen, R., Blinova, V., 2001. Molecular and isotopic characterization of hydrocarbon gas and organic matter from mud volcanoes of the Gulf of Cadiz, NE Atlantic. *Final Proc. Int. Conf. Geological Processes on Deep-Water European Margins*, Moscow, Russia. UNESCO IOC Workshop Report 175, p. 47.
- Stakes, D.S., Orange, D.L., Paduan, J.B., Salamy, K.A., Maher, N., 1999. Cold-seeps and authigenic carbonate formation in Monterey Bay, California. *Mar. Geol.* 159, 93–109.
- Streams, M., Fisher, C.R., 1997. Incorporation of methane by methanotrophic symbionts and symbiont digestion by their host mussel. *Mar. Biol.* 129, 465–476.
- Sweeney, R.E., Kaplan, I.R., 1973. Pyrite framboid formation: Laboratory synthesis and marine sediments. *Econ. Geol.* 69, 618–634.
- Torelli, L., Sartori, R., Zitellini, N., 1997. The giant chaotic body in the Atlantic ocean off Gibraltar. New result from a deep seismic reflection survey. *Mar. Petr. Geol.* 14, 125–138.
- Vázquez, J.T., Somoza, L., Medialdea, T., Maestro, A., Maldonado, A., Vegas, R., 2001. Olistostrome tectonic fronts under the Eurasia-Africa Convergence in the Gulf of Cadiz. *Final Proc. Int. Workshop on the Western Part of Eurasia-Africa Plate Boundary (Azores-Tunisia)*, San Fernando, Spain. *Boletín ROA* No. 3/2001, pp. 132–133.
- Von Rad, U., Roesch, H., Berner, U., Geyh, M., Marchig, V., Schulz, H., 1996. Authigenic carbonates derived from oxidized methane vented from the Makran accretionary prism off Pakistan. *Mar. Geol.* 136, 55–77.